

Mechanisms of Seismically Induced Settlement of Buildings with Shallow Foundations on Liquefiable Soil

Shideh Dashti, M.ASCE¹; Jonathan D. Bray, F.ASCE²; Juan M. Pestana, M.ASCE³; Michael Riemer, M.ASCE⁴; and Dan Wilson, M.ASCE⁵

Abstract: Seismically induced settlement of buildings with shallow foundations on liquefiable soils has resulted in significant damage in recent earthquakes. Engineers still largely estimate seismic building settlement using procedures developed to calculate postliquefaction reconsolidation settlement in the free-field. A series of centrifuge experiments involving buildings situated atop a layered soil deposit have been performed to identify the mechanisms involved in liquefaction-induced building settlement. Previous studies of this problem have identified important factors including shaking intensity, the liquefiable soil's relative density and thickness, and the building's weight and width. Centrifuge test results indicate that building settlement is not proportional to the thickness of the liquefiable layer and that most of this settlement occurs during earthquake strong shaking. Building-induced shear deformations combined with localized volumetric strains during partially drained cyclic loading are the dominant mechanisms. The development of high excess pore pressures, localized drainage in response to the high transient hydraulic gradients, and earthquake-induced ratcheting of the buildings into the softened soil are important effects that should be captured in design procedures that estimate liquefaction-induced building settlement.

DOI: 10.1061/(ASCE)GT.1943-5606.0000179

CE Database subject headings: Centrifuge; Earthquakes; Soil liquefaction; Soil-structure interactions; Settlement; Seismic effects.

Author keywords: Centrifuge; Earthquakes; Liquefaction; Performance-based design; Soil-structure interaction; Settlement.

Introduction

Liquefaction-induced ground deformations depend strongly on cyclic stresses produced by strong shaking and the engineering properties of the liquefiable soil layer. Cyclic and permanent building deformations are also affected by soil-structure-interaction (SSI) effects. The interaction of building deformation with cycles of pore water pressure generation that soften soil response followed by reductions in pore pressure that stiffen soil response is a complex phenomenon. There are presently no well-calibrated design procedures for estimating the combined effects of deviatoric and volumetric-induced building settlement due to cyclic soil softening/stiffening under the static and dynamic loadings of the building. This is in contrast with evaluating liquefaction-induced settlement in the free-field, for which several

widely accepted procedures have been proposed (e.g., Tokimatsu and Seed 1987; Ishihara and Yoshimine 1992).

Three centrifuge experiments were performed to generate well-documented model "case histories" of building response on liquefied ground. In these tests, the input motion, surface motion, ground conditions, ground response, and structural response were closely monitored and documented, thereby providing insight into ground failure and its impacts on structures. The centrifuge tests also shed light on the relative importance of the thickness and density of the liquefiable soil layer, as well as the effects of various building and foundation characteristics on building performance. In each centrifuge test, three structures were placed on a soil profile that contained a layer of liquefiable, saturated Nevada Sand. In this paper, the soil response in the free-field is compared to that observed in the ground surrounding the structures, and the dominant mechanisms of settlement at different locations are identified. The key effects of different testing parameters are discussed to advance the profession's understanding of liquefaction-induced settlement of buildings with shallow foundations.

Current Understanding

Recent earthquakes have provided countless examples of the damaging effects of liquefaction on the built environment. Observations of building performance on liquefied sites include punching settlement, bearing failure, and lateral shifting of buildings. In Niigata, Japan (1964 Niigata Earthquake) and Dagupan City, Philippines (1990 Luzon Earthquake), most of the buildings were two to four stories founded on shallow foundations and supported on relatively thick and uniform deposits of clean sand. For these cases, building settlements were related to foundation dimensions. The confining pressure and shear stress imposed by the buildings

¹Ph.D. Student Researcher, Dept. of Civil and Environmental Engineering, Univ. of California, Berkeley, CA 94702. E-mail: shideh@berkeley.edu

²Professor, Dept. of Civil and Environmental Engineering, Univ. of California, Berkeley, CA 94702 (corresponding author). E-mail: bray@ce.berkeley.edu

³Professor, Dept. of Civil and Environmental Engineering, Univ. of California, Berkeley, CA 94702. E-mail: pestana@ce.berkeley.edu

⁴Associate Adjunct Professor, Dept. of Civil and Environmental Engineering, Univ. of California, Berkeley, CA 94702. E-mail: riemer@ce.berkeley.edu

⁵Associate Project Scientist, Center for Geotechnical Modeling, Univ. of California, Davis, CA 95616. E-mail: dxwilson@ucdavis.edu

Note. This manuscript was submitted on June 28, 2008; approved on June 9, 2009; published online on June 20, 2009. Discussion period open until June 1, 2010; separate discussions must be submitted for individual papers. This paper is part of the *Journal of Geotechnical and Geoenvironmental Engineering*, Vol. 136, No. 1, January 1, 2010. ©ASCE, ISSN 1090-0241/2010/1-151-164/\$25.00.

and their adjacent structures affected building movements, sometimes outweighing other factors (e.g., Tokimatsu et al. 1994). In contrast to these earthquakes, in Adapazari, Turkey (1999 Kocaeli Earthquake), many of the damaged structures were affected by the liquefaction of shallow and relatively thin layers of loose, saturated silt and silty sand. Building settlements were found to be directly proportional to the building's contact pressure, and its height/width (H/B) ratio greatly affected the amount of building tilt and the development of a full bearing capacity failure (Sancio et al. 2004).

Several researchers have used small-scale shaking table and centrifuge tests to study the seismic performance of rigid, shallow model foundations situated atop deep, uniform deposits of saturated, loose-to-medium dense, clean sand (e.g., Yoshimi and Tokimatsu 1977; Liu and Dobry 1997; Hausler 2002). The influence of foundation width on the average settlement of buildings founded on a liquefied sand stratum was recognized by Yoshimi and Tokimatsu (1977) after the Niigata Earthquake and was confirmed by their 1 g shaking table tests and later by the findings of Adachi et al. (1992) after the Luzon Earthquake. Buildings with wider foundations settled less, with all else being equal. Physical model tests also showed that most of the building settlement occurred during strong shaking with a smaller contribution resulting from postshaking soil reconsolidation due to excess pore water dissipation (e.g., Hausler 2002). Foundations settled in an approximately linear manner with time during shaking and settled more than the free-field soil. As a result, building settlements were recognized to be strongly influenced by the structure's inertial forces. Yet, the effects of key parameters on the building's seismic performance have not been well characterized.

Increasing the relative density (D_r) and the overconsolidation ratio of the liquefiable sand layer was shown to decrease the rate of pore pressure generation and seismically induced settlements (e.g., Adalier and Elgamil 2005). The degree of excess pore pressure generation and soil softening was found to depend significantly on the confining pressure and foundation-induced static and dynamic shear stresses. Nevertheless, no clear pattern has been identified for the direction of flow and the degree of soil softening under and around structures as a function of various input parameters. Partial drainage was shown to occur simultaneously with excess pore pressure generation, as fast pore water pressure redistribution took place in a three-dimensional (3D) pattern in response to transient hydraulic gradients (e.g., Liu and Dobry 1997). However, the influence of drainage on building settlements during earthquake strong shaking has not been defined clearly.

The mechanism of void redistribution within a submerged layer of liquefied sand beneath a less pervious layer and the formation of water interlayers (an extreme case of void redistribution) under level ground conditions have been investigated in several physical model studies (e.g., Elgamil et al. 1989; Dobry and Liu 1992; Kokusho 1999). Under mildly sloping ground conditions, shear strain localization occurred at the interface between the loose sand layer and an overlying low permeability layer in numerous centrifuge models. The intensity of shear strain localization depended on initial soil properties, slope-induced static shear stresses, and shaking characteristics (e.g., Fiegel and Kutter 1994; Kulasingam et al. 2004). Nonetheless, the dynamic response of shallow foundations founded on a layered soil deposit of varying hydraulic conductivities that includes a liquefiable soil stratum is not understood adequately.

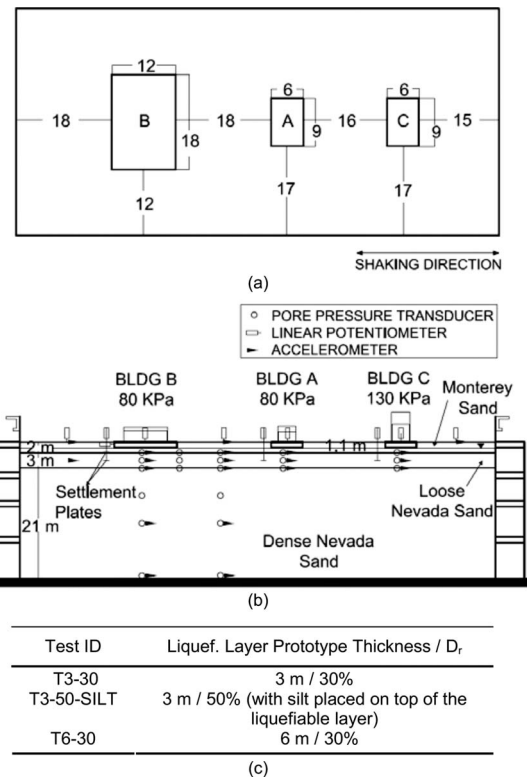


Fig. 1. Centrifuge model layout in experiment T3-30 with most of the approximately 120 transducers omitted for clarity: (a) plan view; (b) cross section view; and (c) centrifuge testing program. All dimensions are given in prototype scale in meters.

Centrifuge Testing Program

A series of three centrifuge experiments were performed to gain insight into the seismic performance of buildings with shallow foundations on a relatively thin deposit of liquefiable, clean sand. Drawings of the first model experiment and a summary of the centrifuge testing program are presented in Fig. 1. The models were spun at a nominal centrifuge acceleration of 55 g, and unless indicated otherwise, all units used in this paper are in prototype scale. Two centrifuge experiments, T3-30 and T3-50-SILT, included a liquefiable soil layer thickness (H_L) of 3 m and nominal relative densities (D_r) of 30 and 50%, respectively. A third experiment (i.e., T6-30), with $H_L=6$ m and $D_r=30\%$, provided information regarding the effect of the liquefiable layer thickness. In T3-50-SILT, the 2-m-thick Monterey Sand on top of the loose Nevada Sand layer was replaced by a 0.8-m-thick layer of silica flour underlying a 1.2-m-thick layer of Monterey Sand. A thorough description of the UC Davis centrifuge geotechnical facilities and instrumentation is provided at their website: <http://nees.ucdavis.edu>. Detailed descriptions of the centrifuge experiments and results are available at the NEES data repository (<https://central.nees.org/>).

The bottom layer of uniform fine Nevada Sand ($D_{50}=0.14$ mm, $C_u \approx 2.0$, $e_{\min} \approx 0.51$, $e_{\max} \approx 0.78$) was dry pluviated to attain $D_r \approx 90\%$. The same Nevada Sand with a D_r of approximately 30 or 50% was then placed by dry pluviation as the liquefiable material. A thin layer of nonplastic silt (silica flour, $D_{50}=0.02$ mm) was placed on top of the looser layer of Nevada Sand in T3-50-SILT to restrict rapid pore pressure dissipation vertically. The silt layer was placed dry in a thin loose lift and was

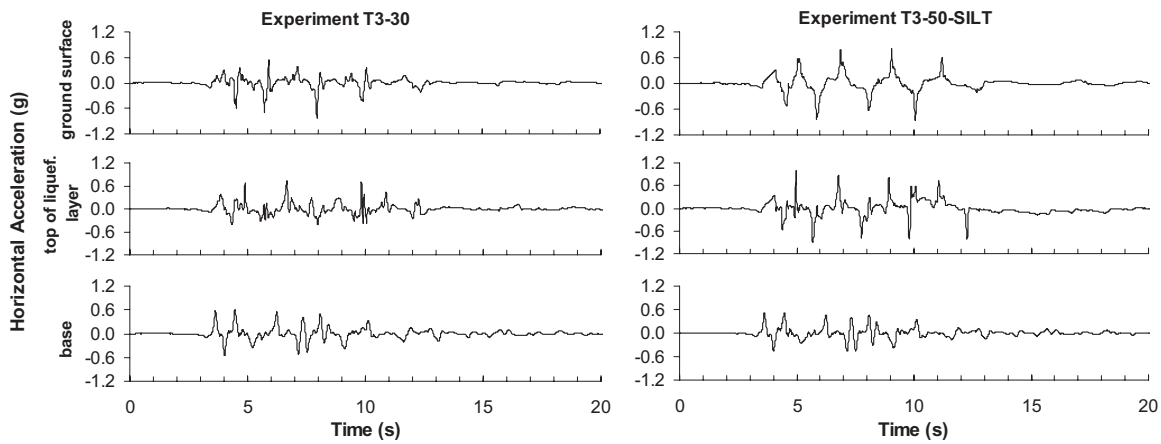


Fig. 2. Vertical arrays of acceleration-time histories recorded in the free-field in experiments T3-30 and T3-50-SILT during the large Port Island event

then lightly compacted with a pressure of about 2 kPa, so that this soil layer was not overconsolidated under the in-flight stresses. Monterey 0/30 Sand ($D_{50} \approx 0.40$ mm, $C_u = 1.3$, $e_{\min} \approx 0.54$, $e_{\max} \approx 0.84$) was placed with a handheld hopper at $D_r \approx 85\%$ as the surficial fill material. The purpose for using this layer was to minimize capillary rise and liquefaction directly below the structures.

The hydraulic conductivities of Nevada Sand and silica flour are approximately 6×10^{-2} and 3×10^{-5} cm/s, respectively (Arulmoli et al. 1992; Fiegel and Kutter 1994). A solution of hydroxypropyl methylcellulose in water was used as the pore fluid with a viscosity of approximately $22(\pm 2)$ times that of water (Stewart et al. 1998). The model was placed under vacuum and then flooded with CO_2 before saturation with the pore fluid. The degree of saturation was checked using in-flight p -wave velocity measurements. The water level was kept at approximately 1.1 m below the ground surface after spinning.

All structural models were single-degree-of-freedom structures with a lumped mass supported by two side columns made of steel, which were placed on a 1-m-thick rigid mat foundation made of aluminum. The structures were designed for static bearing pressures of 80 kPa, 80 kPa, and 130 kPa for Structures A, B, and C, respectively (Fig. 1). Structure A represented a 2-story building (height above ground, $H = 5$ m) with width $W = 6$ m and length $L = 9$ m; Structure B had an increased width and length ($W \times L \times H = 12 \times 18 \times 5$ m); and Structure C represented a taller 4-story building ($W \times L \times H = 6 \times 9 \times 9.2$ m). The fixed-base natural period of the structures ranged from 0.2 to 0.3 s.

Three shaking events were applied to the base of the model. Shaking was applied parallel to the long side of the model. The input motions consisted of a sequence of scaled versions of the north-south, fault-normal component of the ground motion recorded at a depth of 83 m in the Kobe Port Island down-hole array during the 1995 Kobe Earthquake. The “moderate” and “large” Port Island events (with peak base accelerations of about 0.19 and 0.55 g, respectively) were used to study the dynamic response of the structures with slight and significant degrees of liquefaction in the free-field.

Free-Field Response

The free-field response was recorded at locations away from the structures, where there were relatively negligible SSI and bound-

ary effects. Fig. 2 shows a vertical array of acceleration-time histories recorded in the free-field during T3-30 and T3-50-SILT for the large shaking event. Input ground-motion characteristics and initial soil properties greatly influence the rate and extent of soil softening and timing of liquefaction. These factors, in turn, influence the acceleration-time histories experienced within the soil column. The acceleration records in these experiments showed large spikes within the liquefiable Nevada Sand (particularly during the large Port Island event). These large spikes in the acceleration record are associated with the soil’s dilative response above the phase transformation line that result from soil restiffening as the excess pore pressures decrease. The higher relative density of the liquefiable layer in T3-50-SILT led to larger dilation cycles and acceleration spikes compared to T3-30 during the application of large Port Island ground motion.

Fig. 3 presents the recorded excess pore water pressure-time histories at the middepth of liquefiable Nevada Sand in the free-field and the corresponding soil surface settlements in experiments T3-30 and T3-50-SILT during the moderate and large Port Island events. The input base acceleration-time histories are also provided for both events. Positive displacement in these plots indicates settlement, and the plots to the right show the same test data, but with a focus on the early part of strong shaking. Increasing the relative density of the liquefiable Nevada Sand layer from 30 to 50% slowed down the rate of pore water pressure generation at all locations. This effect was greater under the higher confining pressure of structures and during less intense seismic events. Thus, the influence of relative density on the soil’s resistance to pore pressure generation depended on the state of stress and ground-motion intensity. Excess pore pressures generated within the liquefiable layer in the free-field during T3-50-SILT caught up to those in T3-30 after about 2 to 3 s of strong shaking when significant strength loss was reached in both experiments during the moderate and large shaking events.

In experiment T3-30, most of the free-field ground surface settlement occurred after the end of strong shaking, with a decreasing rate as a function of time. Postearthquake settlement rates in the free-field were significantly reduced during T3-50-SILT. This was primarily caused by the presence of the low-hydraulic-conductivity silt layer, which hindered vertical flow and caused long-term horizontal pore pressure migrations from underneath buildings toward the free-field during the large event.

Free-field settlements occurred during strong shaking, suggesting that partial drainage occurred during shaking and the

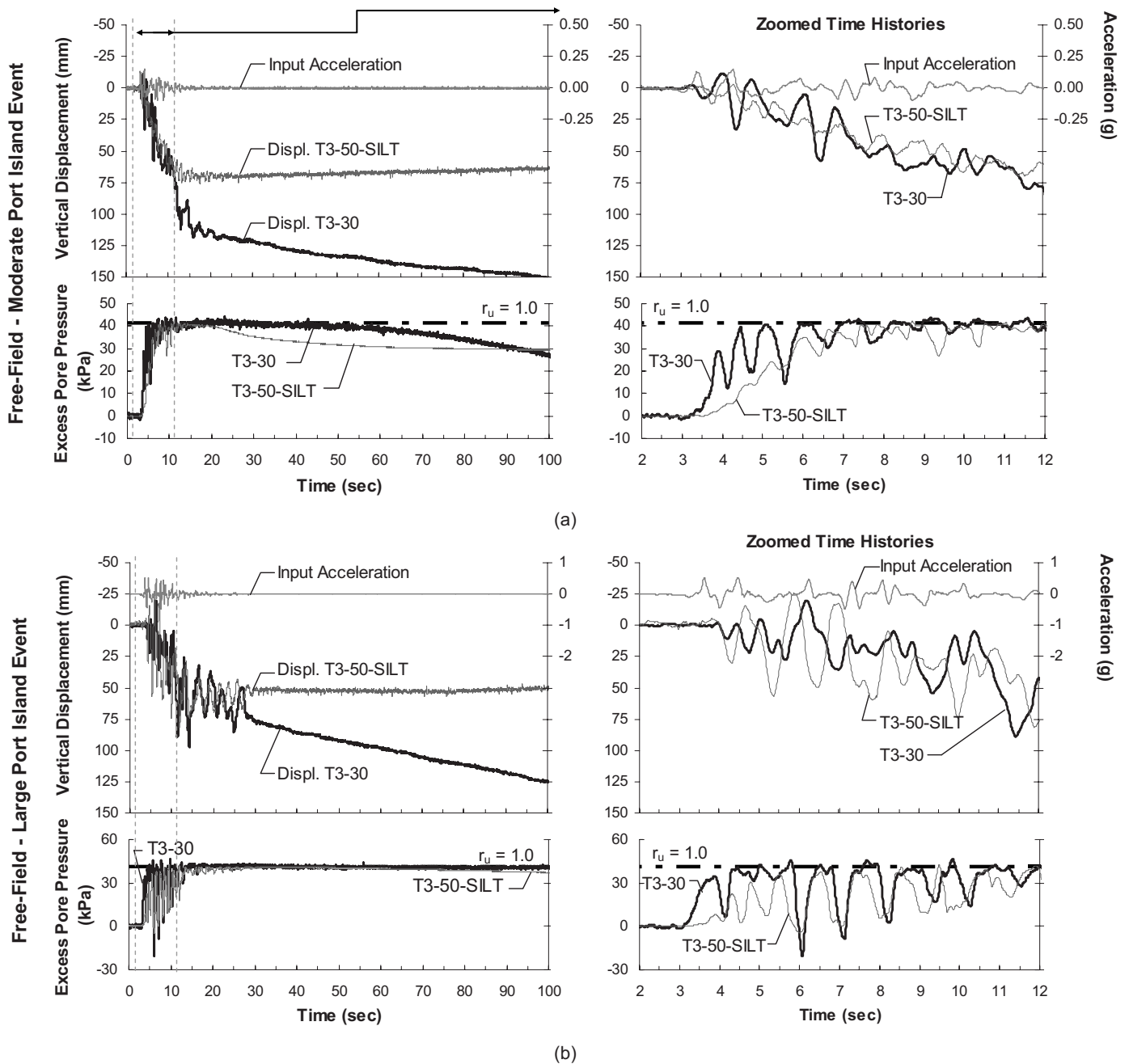


Fig. 3. Excess pore pressure recordings at middepth of the liquefiable layer with the corresponding soil surface vertical displacement-time histories in the free-field in T3-30 and T3-50-SILT during: (a) moderate; (b) large Port Island events

assumption of globally undrained loading is not valid in these experiments. Average free-field settlements in T3-50-SILT were initially similar to those in T3-30, particularly during the large shake, in spite of the presence of silt on top of the liquefiable layer in T3-50-SILT (Fig. 3). The free-field settlements in T3-50-SILT, however, abruptly stopped after strong shaking followed by slow, long-term heave. A possible explanation for the initial settlement response in T3-50-SILT is that as the top of the liquefiable sand settled due to sedimentation and consolidation, it created space for the silt layer on top to expand during loading through the particle settlement phenomenon described in Adalier (1992). As the lower part of the silt seam in the free-field expanded, the weight of the upper, unsaturated Monterey Sand presumably pushed the upper particles of silt into its lower ex-

panding part faster. If the silt layer had not been disturbed by shaking to this point, it became particularly vulnerable to considerable disturbance as the lower sand layers settled and space became available for volumetric expansion, enhancing the breakdown of the silt's solid structure. In addition, the upward migration of water might have caused seepage-induced liquefaction in silt. Under these conditions, the silt layer expanded and settled along with the lower softened layer. This resulted in the initially rapid net surface settlements observed in the free-field. The effective hydraulic conductivity of the silt layer likely approached that of the Nevada Sand during its sedimentation/consolidation phase, until strong shaking ceased. At this point, the silt apparently began to recover its initial hydraulic conductivity and stiffness. However, it is likely that nonlaminar and fast chan-

nel flow (piping) occurred through the silt layer, even after cyclic loading, due to the existing excessive hydraulic gradients, which likely caused cracking.

Empirically based estimates of volumetric reconsolidation settlement in saturated, clean sand (i.e., Tokimatsu and Seed 1987; Ishihara and Yoshimine 1992; and Wu et al. 2003) tended to be slightly greater than the settlements measured within liquefiable Nevada Sand in the free-field. These methods are based on results obtained from undrained cyclic tests on clean sand specimens. The mechanism of a fully undrained cyclic test followed by free drainage does not represent what was observed in these centrifuge tests, where drainage occurred immediately after strong shaking commenced. Additionally, the presence of three structural models in the container resulted in 3D stress nonhomogeneities and lateral water flow that influenced the free-field response.

Response under and around Structures

The recorded excess pore water pressure-time histories at the middepth of the liquefiable layer under each structure as well as the average building vertical displacement-time histories in T3-30 and T3-50-SILT during the moderate and large Port Island events are shown in Fig. 4. Average free-field displacement-time histories are also provided for comparison. Structures began settling after one significant loading cycle with a settlement rate that was roughly linear with time. Building settlements were shown to surpass quickly those measured in the free-field during the large event. Building settlement rates reduced dramatically after the end of strong shaking ($t \approx 12$ s) and became negligible at the end of shaking ($t \approx 25$ s). The observed trends suggest that the contribution of postliquefaction reconsolidation settlements to the total building settlement was relatively minor in these experiments. As a result, other volumetric and deviatoric mechanisms of settlement must have been responsible for the majority of building settlement that occurred during shaking. The apparent link between the initiation and intensity of shaking and the initiation and rate of building settlements point to the importance of a building's dynamic response. Additionally, the influence of partial drainage during earthquake shaking on the responses of the soil and structure cannot be neglected.

Total head isochrones are typically used to measure the direction and magnitude of transient hydraulic gradients formed at different times and the resulting flow tendencies. Fig. 5 compares the transient hydraulic gradients that formed around Structure B in experiments T3-30 and T3-50-SILT during the large Port Island shake. In experiment T3-30, large hydraulic gradients formed vertically upward and horizontally away from the building foundations within the liquefiable layer after 1 to 2 s of strong shaking (during both moderate and large events). Excess pore pressures maintained their peaks throughout strong shaking while oscillating vigorously (Figs. 3 and 4). After the end of strong shaking, a rapid reduction in excess pore pressures underneath the structures was observed for approximately 20 s. This response was expected, as no significant excess pore pressures were being generated during this time and the 3D hydraulic gradients were near their peak values. After both vertical and horizontal hydraulic gradients declined, slower upward vertical pore pressure dissipation began to control the flow under buildings until pore water pressures approached the hydrostatic condition.

In experiment T3-50-SILT, upward flow from the lower dense layer of Nevada Sand began after about 2 s of shaking. As expected, smaller excess pore pressures were generated within the

liquefiable layer in T3-50-SILT ($D_r \approx 50\%$) compared to T3-30 ($D_r \approx 30\%$) under the confining pressure of structures, particularly during the moderate shake. The largest excess pore pressures within the liquefiable layer were measured at shallower depths in T3-50-SILT during both seismic events. This pattern indicated a tendency for void redistribution under structures due to the presence of the silt layer. The resulting 3D hydraulic gradients led to a quick but small drop in excess pore pressure measurements within the liquefiable layer under the structures after strong shaking as pore pressures attempted to stabilize horizontally. This drop was followed by a relatively slow increase in excess pore pressures within the liquefiable layer for 50 to 70 s before they started to decline as water traveled upward from the lower dense layer of Nevada Sand. During this time, horizontal gradients became negligible and the highly disturbed silt layer around the footings likely started to regain its strength. In summary, a comparison of the flow potential in the two experiments indicated a stronger tendency for drainage and volumetric strains associated with drainage under structures during experiment T3-30 compared to T3-50-SILT.

Greater net excess pore pressures developed within the liquefiable soil under Structure B (with the largest foundation contact area) compared to Structures A and C (Fig. 4). The building pressure over a wider area led to a higher capacity for excess pore pressure generation in a larger volume of soil under and around the mat. Smaller excess pore pressures were generated within the liquefiable Nevada Sand under Structure C, which had the largest foundation contact pressure and H/B ratio compared to the other two structures. Although sand under higher confinement has the capacity to generate higher excess pore pressures (for a given pore pressure ratio, $r_u = u_e / \sigma'_{vo}$, where u_e is the excess pore water pressure and σ'_{vo} is the initial overburden effective stress), it also requires more energy to develop excess pore pressures. The response of Nevada Sand under the large confining pressure of Structure C may be partially explained by its higher resistance to pore pressure generation under the selected input motions and partially by the relatively small contact area of the footing facilitating more efficient dissipation of excess pore pressures.

Table 1 presents a comparison of the average vertical movements of the structures relative to those in the free-field at different times during T3-30 and T3-50-SILT. The building settlements minus the free-field settlements in experiment T3-30 were significantly greater than those in T3-50-SILT immediately after strong shaking during the moderate event. These relative settlements continued to stay larger in T3-30 with the exception of Structure C. Although Structure C settled less during experiment T3-30 compared to T3-50-SILT, it showed a stronger tilting tendency in T3-30. The higher relative density of the liquefiable Nevada Sand in T3-50-SILT delayed the development of high excess pore pressures under structures and its greater dilative tendencies arrested movements earlier during the moderate shake.

As shown in Fig. 4 and Table 1, the pore pressure response under the structures as well as the relative settlement of buildings with respect to the free-field in experiments T3-30 and T3-50-SILT became more similar under more intense shaking (i.e., large Port Island event). A denser soil (particularly under the higher confining pressure of the structures) requires more energy to generate excess pore pressures and to cause significant void redistribution. However, during the large Port Island event, the energy of the ground motion was sufficiently intense to develop significant pore water pressures at most locations in both experiments. More intense shaking is also expected to increase the potential for significant void redistribution and strain localization at the sand/silt

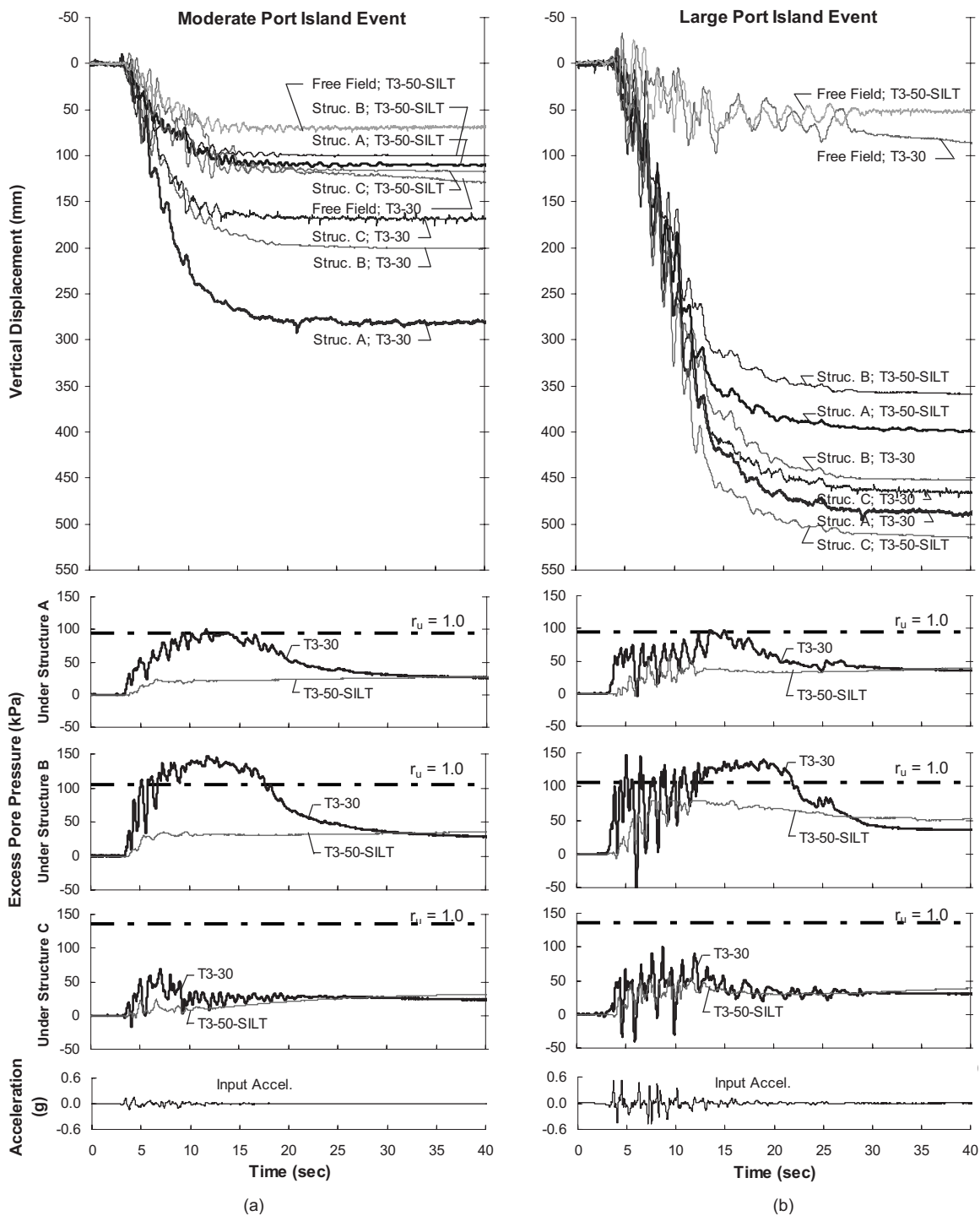


Fig. 4. Excess pore pressure recordings at the middepth of the liquefiable layer under each structure in addition to average building vertical displacement-time histories in T3-30 and T3-50-SILT during: (a) moderate; (b) large Port Island events

interface if all else remained equal. This explains the large building movements relative to the free-field that were observed during the large Port Island event in T3-50-SILT.

In contrast to the displacement patterns observed in the free-field, approximately $98 \pm 1\%$ of total building settlements in T3-30 occurred during shaking. Postshaking structural settlements were completed within 50 to 70 s in this experiment, after which buildings essentially stopped moving. In experiment T3-50-SILT, on the other hand, the presence of the low-permeability silt layer on top of liquefiable Nevada Sand increased the contribution of

postearthquake structural settlements. The structures achieved approximately $90 \pm 5\%$ of their total permanent displacements during shaking in T3-50-SILT, while around $5 \pm 2\%$ of their total displacements still remained 170 s after the end of shaking. In addition to slower volumetric settlements caused by slower flow, void redistribution within Nevada Sand that was capped by silica flour likely reduced the soil's resistance to static building loads for an extended time after shaking stopped. This led to additional postearthquake building settlements during T3-50-SILT.

Settlement trends observed in the two experiments and two

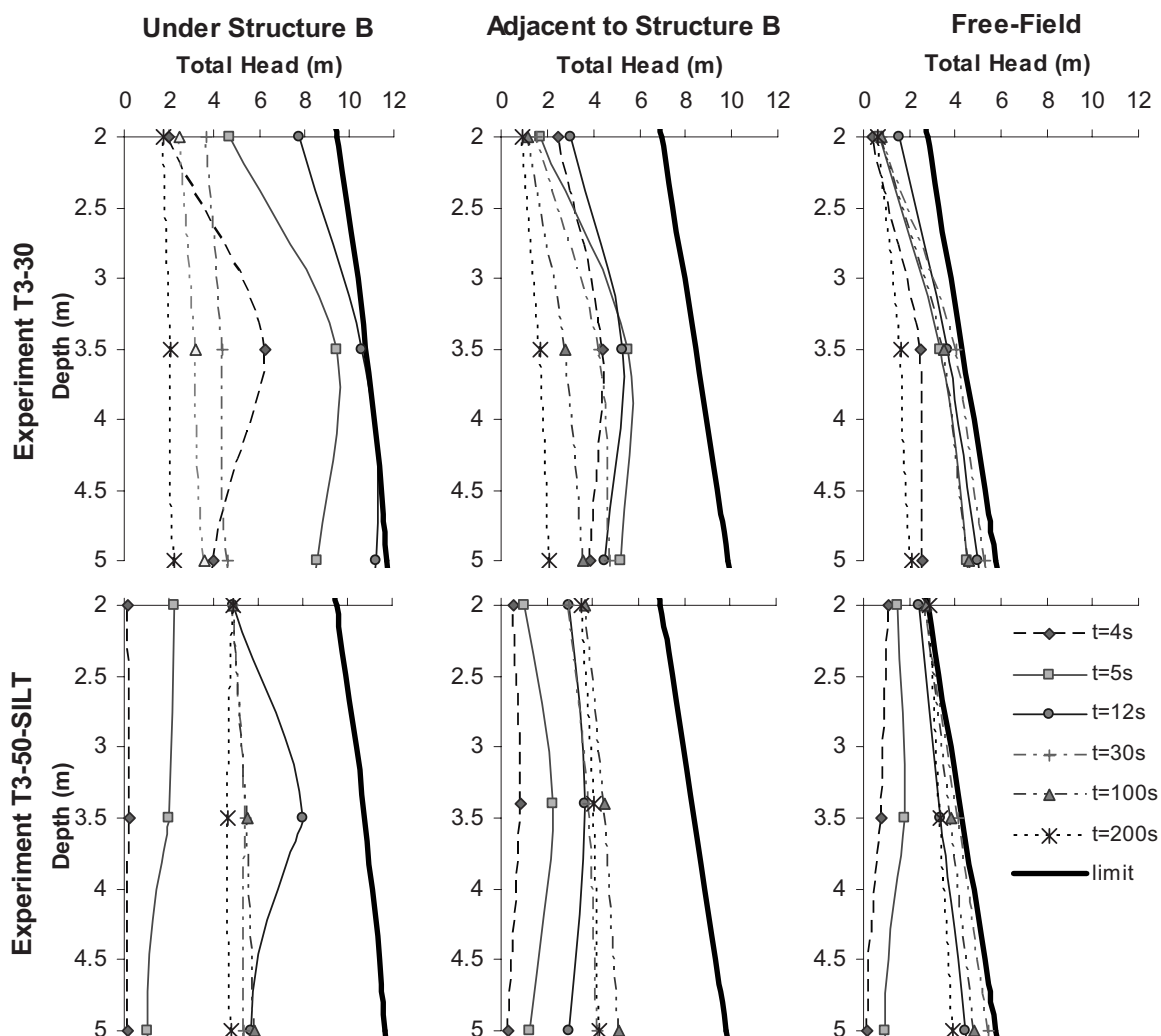


Fig. 5. Representative total head isochrones measured within the liquefiable layer during the large Port Island event in T3-30 and T3-50-SILT. (Note: the limit total head in these figures indicates $r_u=1.0$; $t \approx 3$ s corresponds to the beginning of shaking.)

shakes were consistent for structures that did not have high tilting tendencies (i.e., Structures A and B with low height to width ratios, H/B). Structure A settled slightly more than B in all cases, and they both settled less during T3-50-SILT compared to T3-30.

Therefore, increasing the foundation contact area or the relative density of the liquefiable material decreased total permanent building settlements in these experiments. The response of Structure C was more difficult to predict, because SSI-induced shear

Table 1. Average Vertical Movement of Structures Relative to Those in the Free-Field at Different Times during T3-30 and T3-50-SILT for the Moderate and Large Port Island Events

Shaking event	Experiment	Structure	Structural settlement relative to free-field		
			$t=12$ s	$t=30$ s	$t=1000$ s
Moderate Port Island	T3-30	A	175	200	150
	T3-50-SILT	A	35	40	50
	T3-30	B	100	120	70
	T3-50-SILT	B	35	30	40
	T3-30	C	85	90	35
	T3-50-SILT	C	40	50	55
Large Port Island	T3-30	A	260	410	330
	T3-50-SILT	A	265	345	370
	T3-30	B	235	375	290
	T3-50-SILT	B	210	305	330
	T3-30	C	275	385	305
	T3-50-SILT	C	360	460	485

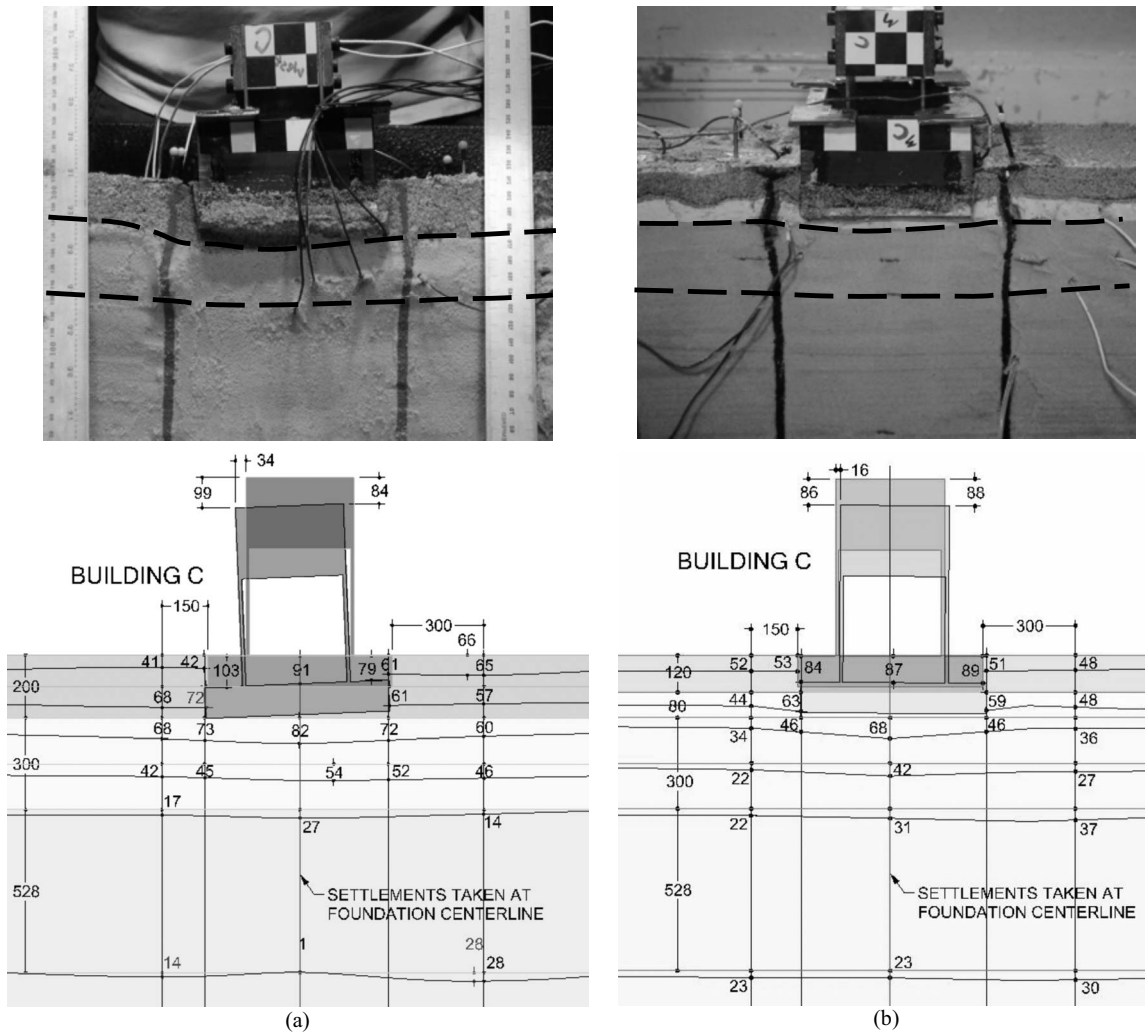


Fig. 6. Representative photographs and drawings showing the total permanent horizontal deformation of colored sand columns adjacent to Structure C and the vertical displacement of colored sand rows at different depths in the vicinity of Structure C after model excavation in: (a) T3-30; (b) T3-50-SILT. (Note: all numbers in the drawings are in prototype scale centimeters.)

stresses were more important due to its larger contact pressure and higher center of gravity. Structure C settled slightly less than Structure A during the large shake in T3-30 but settled significantly more than the other structures in T3-50-SILT. A building's response to rocking is highly sensitive to the changes in building shaking and soil softening. Also, an increase in soil relative density in these cases might have an adverse effect on building settlements by amplifying the acceleration response. In fact, Structure C settled more in T3-50-SILT than in T3-30 during the large Port Island earthquake likely due to its amplified SSI-induced ratcheting into the softened foundation soil.

Results of previous physical model tests on mildly sloping saturated sand, without a sudden spatial variation in hydraulic conductivity, have shown lateral deformations to be distributed throughout most of the depth of the liquefiable layer, increasing from the bottom to the surface (e.g., Fiegel and Kutter 1994; Kulasingam et al. 2004). The presence of a low hydraulic conductivity layer in the sloping ground experiments, however, resulted in a concentration of lateral displacements below the sand/silt interface. This is due to primarily the loosening of the interfacial soil because of sedimentation/consolidation of the lower sand material. Similar patterns of response were observed in this study's experiments under the static and dynamic shear

stresses imposed by the buildings. As shown in Fig. 6, lateral movements of the colored sand columns adjacent to the structures were mostly evenly distributed throughout the liquefiable layer in T3-30; whereas they were largely concentrated below the Nevada Sand/silica flour interface in T3-50-SILT. Additionally, large lateral movements of colored sand columns adjacent to the structures in both experiments attest to the significance of deviatoric-induced soil deformations underneath buildings, which are ignored by the available design procedures.

Representative settlement patterns from measurements made during model dissection after all testing was completed are also shown in Fig. 6. Most of the deformation occurred in the liquefiable sand layer as anticipated, with structures settling more than the adjacent ground and the ground adjacent to structures settling more than the free-field. Fig. 5 showed larger net excess pore pressure and total head measurements under and near structures compared to the free-field in both experiments during the large event (particularly during T3-30). This led to a stronger tendency for outward flow near the structures and localized volumetric strains due to partial drainage during loading. Larger settlements observed adjacent to the structures compared to the free-field indicate that the net increase in localized volumetric settlements due to partial drainage near the perimeter of foundations must have

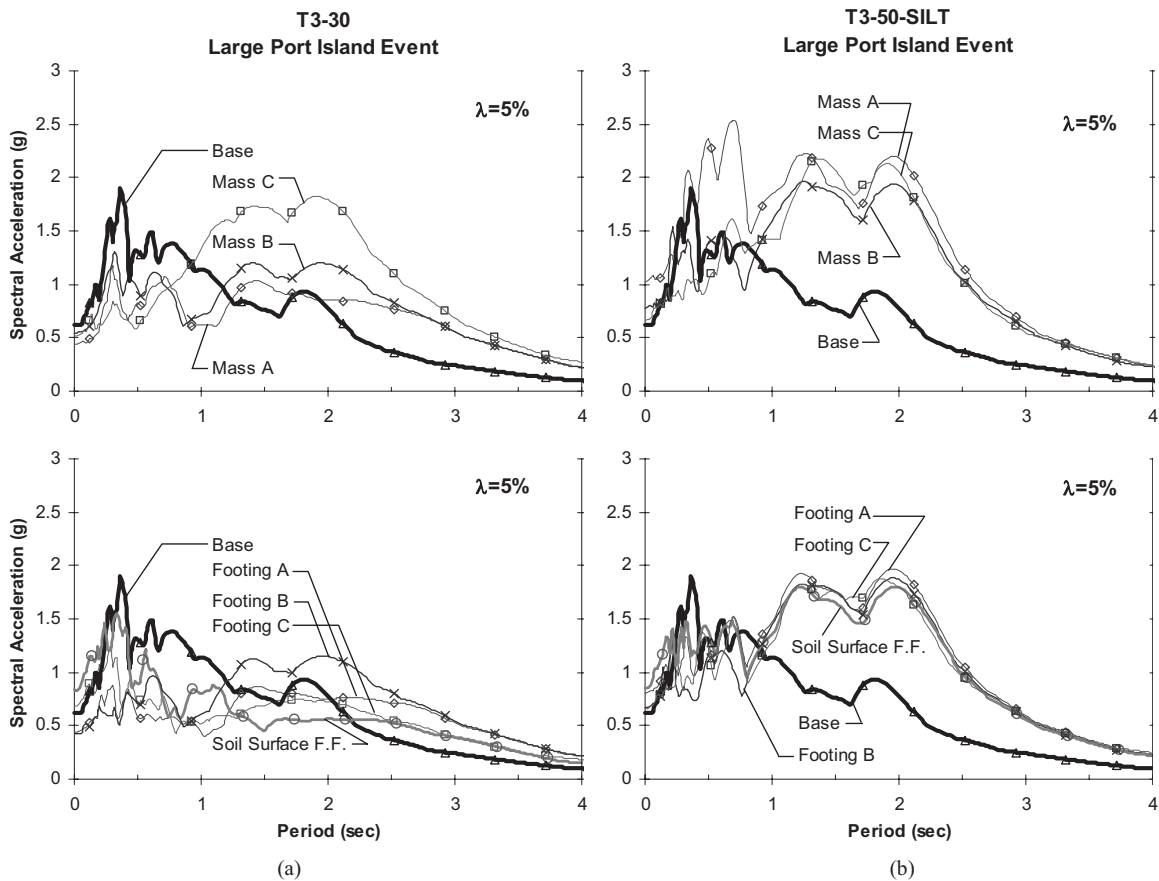


Fig. 7. Acceleration response spectra (5% damped) of horizontal ground motions recorded on the foundation and mass of the structural models and the base of the container during the large Port Island event in: (a) T3-30; (b) T3-50-SILT

been larger than the heaving effect due to constant-volume building-induced shearing in these model experiments.

Fig. 7 presents the acceleration response spectra (5% damped) of horizontal motions recorded on the base of the container (input motion), the soil surface in the free-field, and on the footing and lumped mass of the structural models in T3-30 and T3-50-SILT during the large Port Island event. The initial site periods of the soil deposits in these centrifuge tests were both around 0.3 s, while the fixed-base natural period of the structures ranged from around 0.2 to 0.3 s. During the large shake in experiment T3-30, foundation horizontal accelerations were mostly deamplified at periods of less than about 1.2 s, with the exception of a few high frequency peaks that were produced by dilation cycles of the liquefied soil. In T3-30, Building C, with the highest H/B ratio, experienced the largest spectral amplification among the structural masses. Foundation horizontal accelerations were significantly amplified at periods of greater than 1 s during T3-50-SILT, leading to greater spectral values of the structural masses, which were generally similar for different structures.

Discussions on Liquefaction-Induced Building Settlement Mechanisms

The normalized average permanent building settlements measured during the large Port Island event in three centrifuge model tests are shown in Fig. 8. Results from available case histories and two previous centrifuge experimental studies are also included in this figure. The building settlements shown in Fig. 8 were esti-

mated as the total settlement of structures minus the average settlement of the lower deposit of dense Nevada Sand during the corresponding earthquake. Settlements were then normalized by the initial thickness of the liquefying layer (H_l).

The results of T6-30, where the liquefiable layer was relatively

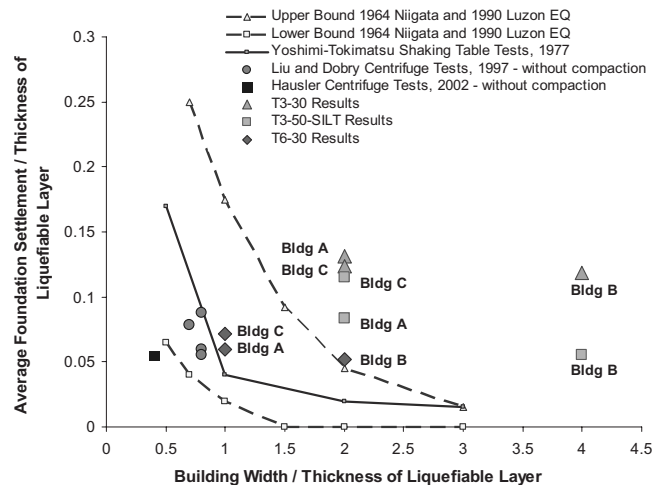


Fig. 8. Normalized foundation settlements measured in the three centrifuge experiments performed in this study during the large Port Island event compared to the available case histories and previous physical model tests

Table 2. Primary Mechanisms of Ground and Building Displacement

Displacement type	Mechanisms of displacement	Strain abbreviation	Location
Volumetric	(a) Localized volumetric strains due to partial drainage	ϵ_{p-DR}	All locations
	(b) Sedimentation after liquefaction	ϵ_{p-SED}	
	(c) Consolidation due to excess pore pressure dissipation	ϵ_{p-CON}	
	(d) Volumetric expansion due to decrease in effective stresses	ϵ_{p-EXP}	
	(e) Settlements due to the compression of air in a partially saturated soil or due to compliance errors	ϵ_{p-COMP}	
Deviatoric	(a) Partial bearing failure due to strength loss in the foundation soil	ϵ_{q-BC}	Under and adjacent to structures
	(b) SSI-induced building ratcheting due to cyclic loading of foundation	ϵ_{q-SSI}	

thick (i.e., $H_L=6$ m), were consistent with the results from previous centrifuge tests and case histories involving deep deposits of liquefiable materials. The results of T3-30 and T3-50-SILT, where the liquefiable layer was relatively thin (i.e., $H_L=3$ m), were not consistent with other test results and observations. If there is a sufficient thickness of liquefiable soil present at a site, significant liquefaction-induced building settlements can occur that are not proportional to the thickness of the liquefying layer. These results indicate that normalizing building settlement by the thickness of the liquefiable layer is misleading in understanding the response of different structures founded on relatively thin, shallow deposits of saturated granular soils. Therefore, this widely used normalization should not be employed in engineering practice. The results also highlight the need for a better understanding of the primary factors influencing liquefaction-induced building settlements.

As was shown in Fig. 4, all structures began to settle rapidly after one significant loading cycle, quickly surpassing settlements in the free-field in both experiments. Fig. 5 showed a strong tendency for horizontal flow away from underneath the buildings soon after shaking began during experiment T3-30, which influenced the soil's and structure's seismic responses. The slower rate of pore pressure generation underneath structures and smaller flow tendencies away from the foundations in T3-50-SILT compared to T3-30 did not appear to affect notably the initiation of building movements during the large shake, as buildings started to settle similarly in the two experiments (Fig. 4). Fig. 7, however, showed that the higher relative density and stiffness of the liquefiable soil in T3-50-SILT increased the cyclic inertial forces of structures compared to experiment T3-30. Although affected by the extent of soil softening, the initial building settlements in these experiments were more in phase with their acceleration response. The rates of building settlements slowed down dramatically after strong shaking ceased. The settlement rates after strong shaking, however, remained larger in T3-30 compared to T3-50-SILT with a higher degree of softening in the underlying soils. Additionally, Fig. 6 showed large horizontal movements within the liquefiable layer underneath structures proving the presence and importance of deviatoric-type movements under the static and dynamic shear stresses induced by the buildings.

It has been shown through previous case studies and physical model tests that seismically induced cyclic pore water pressure generation and liquefaction (i.e., $u_e \cong \sigma'_{vo}$) may produce or intensify several mechanisms of settlement, which can damage structures as well as surrounding utilities. Deformations resulting from earthquake loading may be categorized as either volumetric- or deviatoric-induced deformations. Based on the experimental results and observations presented in the previous sections, Table 2 lists the primary settlement mechanisms that were potentially ac-

tive in this study. The volumetric and deviatoric strains that develop at any location are a function of the interactions between free-field and structure-induced cyclic demands as well as static shear stresses imposed by the foundation. Volumetric-induced settlement mechanisms include:

- Localized volumetric strains during partially drained cyclic loading controlled by 3D transient hydraulic gradients;
- Settlements due to sedimentation or solidification after liquefaction or soil structure break-down;
- Consolidation-induced volumetric strains as excess pore pressures dissipate;
- Expansion or swelling of soil structure due to decrease in effective stresses; and
- Settlements caused by the compressibility of pore air in a partially saturated soil or caused by compliance errors in physical model testing.

Deviatoric soil deformations near a structure can be critical, particularly at high shaking levels. They depend on static driving shear stresses caused by the foundation bearing loads ($\alpha = \tau/\sigma'_{vo}$) and the SSI-exacerbated cyclic loads, as well as soil properties. Deviatoric-induced settlement mechanisms include:

- Partial bearing failure under the static load of structures due to strength loss in the foundation soil resulting in limited punching settlements or tilting of the structure.
- Cumulative foundation settlements due to SSI-induced cyclic loading near the edges of the footing.

The response and contribution of each of these settlement mechanisms to total building displacements are expected to be a function of soil and structural properties and ground motion characteristics. The identified settlement mechanisms and the influence of critical testing parameters on each are discussed in the following sections.

Volumetric Deformation Modes

Localized Volumetric Strains during Partially Drained Cyclic Loading

It is often assumed that the response of saturated sands is fully undrained during earthquake shaking, while all drainage is accounted for after the end of shaking. Results of previous case studies and experiments as well as these centrifuge tests indicate that saturated sand does not respond in a fully undrained manner during earthquake loading. Local pore water migrations start as soon as hydraulic gradients form. The soil's hydraulic conductivity increases as it liquefies (e.g., Jafarzadeh and Yanagisawa 1995), which further increases the potential for drainage during cyclic loading. Consequently, cyclic shear-induced localized volumetric strains due to pore water pressure migration/redistribution

are expected to occur during strong shaking. Furthermore, Vaid and Eliadorani (1998) showed that saturated sand (both contractive and dilative under fully undrained or drained loading) can experience strain softening through partially drained cyclic loading.

The contribution of this settlement mechanism to the total movements at a given location depends on the magnitude of the 3D hydraulic gradients and the soil's hydraulic conductivity. The ground-motion characteristics, soil layering, initial soil properties, the 3D state of stress across the model, and dynamic SSI effects all influence the transient hydraulic gradients across the model, which lead to flow and the subsequent localized volumetric strains during loading.

Settlements due to Sedimentation

Immediately after significant strength loss, the uppermost part of the liquefiable sand is in a state of dispersion. The settling particles accumulate at the bottom to form a solidified zone. This zone increases in thickness with time and concurrently consolidates under its own weight. Solidification generally advances from the base of the liquefied soil up immediately after significant strength loss, when the excess pore water pressures begin to return to hydrostatic (Adalier 1992).

Through simple shear tests on saturated sand, Nagase and Ishihara (1988) found that volumetric strain during consolidation was uniquely correlated to the excess pore water pressure ratio (r_u) as long as $r_u < 1.0$. These volumetric strains were approximately linearly proportional to the cyclically induced excess pore water pressures. When the condition of $r_u = 1.0$ was approached, a sharp increase in volumetric strains was observed, a condition attributed to sedimentation. The magnitude of sedimentation-induced volumetric strains relies on the extent of soil skeleton breakdown beyond the point of initial liquefaction. The disturbance energy experienced by the sand particles may be represented by the maximum shear strains within the soil profile (Adalier 1992). Therefore, sedimentation was correlated to the maximum shear strains representing the level of disturbance in the soil skeleton.

Settlements due to Consolidation

Consolidation is a time-dependent deformation that occurs as pore water pressures in excess of hydrostatic dissipate and the soil's effective stress increases. In the case of liquefaction, consolidation primarily occurs when a continuum soil-skeleton is formed (after sedimentation). As the net amount of excess pore pressure reduces in the solidified layer, the degree of particle contact forces increases, leading to permanent volumetric strains as the solidified soil structure consolidates. Consolidation-induced settlements start locally immediately after pore water pressures are generated at a given location and achieve their highest rate when the difference between the rate of outward flow and the rate of seismically induced pore pressure generation is greatest. This is expected to occur immediately after strong shaking, when hydraulic gradients are at their peak and pore pressure generation slows down considerably. SSI-induced cyclic shear stresses in the soil layers near and below the foundations should be added to free-field cyclic stresses ratio ($CSR_{\text{free-field}}$) when estimating the extent of pore pressure generation and consolidation-induced settlements under a structure. In addition, there is a minor adverse K_σ effect due to the increase in vertical effective stresses underneath buildings compared to the free-field, which should be taken into account in estimating the soil resistance to liquefaction [cyclic resistance ratio (CRR)].

If the average total stresses are assumed to be constant during the seismic excitation, then consolidation-induced volume changes can be related to changes in the net excess pore pressure with time caused by generation and simultaneous dissipation/redistribution (e.g., Pestana et al. 1997). The rates of net excess pore pressure dissipation and consolidation-induced settlements during shaking are controlled by ground-motion characteristics, initial soil properties (particularly relative density and coefficient of consolidation), and the 3D stress state in the model. The net rate of excess pore pressure dissipation may also influence the magnitude of consolidation-induced settlements during cyclic loading, as faster net outflow would lead to more consolidation while large hydraulic gradients are maintained during strong shaking. Postearthquake consolidation-induced settlements, however, are not affected by the rate of pore pressure dissipation, and are only influenced by the net value of excess pore pressures at the end of cyclic loading and the coefficient of volume change (m_v). The compressibility of a sandy soil depends primarily on its initial relative density and the effective confining stress.

Expansion of Soil Structure due to Decrease in Effective Stresses

Local expansive volumetric strains may occur in different soil layers caused by increased pore water pressures and reduced effective stresses during shaking before the soil structure begins to breakdown near liquefaction. Various testing parameters that lead to the generation of higher net excess pore pressures within the soil at a given location increase the contribution of this mechanism to the total displacements. However, it is not typically a dominant settlement mechanism.

Settlements Caused by the Compressibility of Pore Air in a Partially Saturated Soil or Compliance Errors

It is difficult to achieve 100% saturation in a large centrifuge model. It is also reasonable to assume at some field sites the foundation soil could be only partially saturated. Some volume change could potentially occur during the application of dynamic loading in a partially saturated model due to the compressibility of pore air. As the degree of saturation reduces, volumetric settlements during loading tend to increase and the volume change during postliquefaction drainage is expected to decrease (Sawada et al. 2006). Even a small departure from full saturation could result in noteworthy settlements of a relatively thick soil layer. However, movements within the liquefiable layer of Nevada Sand due to the compression of pore air do not tend to contribute significantly to the total displacements at the soil surface in these tests because of the limited thickness of this layer. The thicker layer of dense Nevada Sand settled during shaking, perhaps partially due to lack of full saturation and compliance errors in combination with rapid vertical drainage of pore fluid toward the surface. This settlement mechanism may have influenced the initial movements observed across the model before significant strength loss was achieved. Stronger shaking and a larger volume of void space within the soil profile (soil in a looser state) increase the contribution of this settlement mechanism to total displacements. It is not likely for this mechanism to contribute significantly to liquefaction-induced settlements at building sites with shallow water tables in the field.

Deviatoric Deformations

Partial Bearing Capacity Failure due to Strength Loss

Stiffness and strength loss in the foundation material can result in punching settlement of structures or building tilt. Limited punch-

Table 3. Effects of Key Parameters on the Dominant Displacement Mechanisms, Assuming a Shallow Liquefiable Layer Underlying a Large Mat Foundation

Increase in parameter	Primary deformation mechanisms ^a				
	ϵ_{p-DR}	ϵ_{p-SED}	ϵ_{p-CON}	ϵ_{q-BC}	ϵ_{q-SSI}
Peak ground acceleration (PGA)	↑↑	↑↑	↑↑	↑↑	↑↑
Liquefiable layer relative density (D_r)	↓↓	↓↓	↓	↓↓	↓
Liquefiable layer thickness (H_L)	↑	↑	↑↑	↑	↓
Foundation width (B)	↓	↓	↑	↑	↓↓
Static shear stress ratio, $\alpha = \tau_{static} / \sigma'_{vo}$	↓	↓	↓	↓↓	—
Structure height/width ratio (H/B)	↑	↑	↑	—	↑↑
Building weight	↑↓	↑↓	↑↓	↓	↑↑
3D drainage	↑↑	↓	↑	↓	↓

^aThe direction of the arrows indicates the impact on the magnitude of the strain value for an increase in the parameter, and the number of arrows indicates the relative importance of that parameter. Double-sided arrows indicate that both directions are possible depending on the specific testing conditions.

ing or tilting is generally associated with conditions in which postliquefaction strengths are sufficient to prevent complete bearing failure. These settlements occur after cyclic softening, until adequate dilation-induced restiffening develops to stop further movements. Additionally, as the soil liquefies rapidly in the free-field (within 1 to 2 s of shaking in these tests), even a nonliquefied soil under the static shear stresses imposed by a heavy structure can lose its lateral support and deform horizontally away from underneath the building foundation.

In addition to seismically induced soil strength loss, rapid upward migration of water from the softened deposit may further reduce the strength of the surface soil and the upper portion of the liquefiable layer. This upward flow may even generate seepage-induced liquefaction, causing additional large deformations or loss of bearing capacity under the structures (e.g., Martin et al. 1975), which may continue long after strong shaking. In the presence of a low permeability layer on top of liquefiable sand, void redistribution and volumetric expansion are expected below the interface, leading to a higher potential for shear strain localization and partial bearing failure of structures during intense shaking.

Settlements due to SSI-Induced Cyclic Loading of the Foundation

Shear-induced structural settlements (i.e., ratcheting) may occur due to SSI-induced cyclic loading of the foundation (i.e., differential horizontal inertial forces between the foundation and the ground as well as vertical loading pulses due to structural rocking). Uplift of the opposite edge of the foundation disturbs the soil underneath it so that the next cycle of downward loading at this location induces more settlement. This mechanism results in a cumulative settlement of buildings and may occur with or without soil liquefaction. Its role, however, depends on and interacts with the extent of strength loss in the foundation soil. Through this mechanism, the structure settles violently during strong shaking by horizontally displacing the weakest underlying soil stratum away from the footing. The structural vibration and movement simultaneously intensifies pore water pressure generation in the foundation soil, which in turn exaggerates other mechanisms of settlement (i.e., ϵ_{p-DR} , ϵ_{p-SED} , ϵ_{p-CON} , and ϵ_{q-BC}).

The timing and location of soil strength loss in the foundation material are expected to strongly influence the accelerations at the foundation level and the SSI-induced cyclic loads, which would again interact with the soil response around the foundation. Thus, the SSI-exacerbated cyclic shear stresses around a foundation interact with cyclic softening/restiffening in the underlying soil, further affecting the limited punching/bearing settlements of structures as well as the volumetric settlement mechanisms.

Effects of Key Parameters on Liquefaction-Induced Settlement Mechanisms

Examination of the trends in the results obtained from the three centrifuge tests enabled a qualitative assessment of the effects of some key parameters on liquefaction-induced settlements. Table 3 qualitatively describes the influence of several key parameters on the dominant mechanisms involved in liquefaction-induced building settlement. The direction of the arrows in Table 3 indicates an increase or decrease of the strain value. The number of arrows indicates the relative importance of that particular parameter. Further study is warranted for a more quantitative evaluation of the role of each parameter.

Seismic Demand

Increasing the intensity and duration of the ground shaking amplifies the intensity and duration of cyclic shear stresses that generate larger excess pore pressures, leading to a faster and more extensive breakdown of the sand structure. Thus, increasing the seismic demand intensifies all of the mechanisms of settlement identified through these experiments. It is one of the most important parameters. Ground motion characteristics also affect the influence of other parameters, such as soil relative density, static shear stress ratio, and structural H/B ratio, on the deformation mechanisms. The effects of increasing ground motion intensity on some of the dominant building settlement mechanisms may reach a limit, after which building settlement rate is expected to plateau.

Sand Initial Relative Density

Denser sand exhibits a greater resistance to seismically induced pore pressure generation and strength loss and has a smaller void space available for volumetric compaction. As a result, sand at a higher relative density is expected to undergo smaller volumetric settlements. However, this effect is influenced strongly by the characteristics of the structure and the ground motion. Denser sand with higher stiffness and resistance to softening also increases the factor of safety against bearing failure of the structure (i.e., smaller ϵ_{q-BC}). The greater soil stiffness, however, amplifies the dynamic demand imposed on the structures, which may amplify SSI-induced building ratcheting (ϵ_{q-SSI}), depending on the fundamental period of the site and structure.

Liquefiable Layer Thickness

Increasing the thickness of the liquefiable layer is anticipated to intensify all volumetric-induced settlement mechanisms by increasing the volume of the soil that undergoes large strains. A thicker liquefiable soil layer might, however, deamplify accelera-

tions at the foundation level, depending on the fundamental period of the site and structure, and hence, reduce SSI-induced building ratcheting (ϵ_{q-SSI}). Depending on the properties of the site, structure, and ground motion, if there is a sufficient thickness of liquefiable soil under the foundation, further increases in the thickness of the liquefiable soil likely have a marginal impact on building settlements.

Foundation Width

Wider foundations reduce the ability of seismically induced excess pore water pressures to dissipate rapidly from underneath structures by increasing the drainage path (if all else remains equal). This longer drainage path may result in larger and more sustained net excess pore pressures under wider structures. Hence, a wider building might amplify the contribution of sedimentation- and postshaking consolidation-induced settlements (ϵ_{p-SED} and ϵ_{p-CON}) under the building. Similarly, wider structures are likely less influenced by localized volumetric strains due to drainage near the edges of the foundation (ϵ_{p-DR}). Considering immediate settlement procedures for static loading, building settlements related to the ϵ_{q-BC} mechanism should increase as foundation width increases. However, a wider mat foundation is expected to reduce the amount of SSI-induced deviatoric deformations (i.e., ϵ_{q-SSI}), because a wider foundation is expected to rock less. It is also more difficult to push soil out laterally from underneath a wider building to accommodate its cumulative downward movement.

Static Shear Stress Ratio

Generally, excess pore pressure ratio (r_u) values of near 1.0 are required for large volumetric strains associated with particle sedimentation to occur under essentially zero effective stress. The increase in the static shear stress ratio ($\alpha = \tau_s / \sigma'_{vo}$) in a soil makes it difficult to reach the state of zero effective vertical stress, unless the cyclic shear stresses are large enough to reduce the net shear back to zero. Hence, the presence of static driving shear stresses (near the perimeter of structures) is expected to reduce the potential for sedimentation-induced settlements (ϵ_{p-SED}).

Increasing the static shear stress ratio is expected to increase the soil resistance to cyclic pore pressure generation (decreasing the contribution of ϵ_{p-CON} and ϵ_{p-DR}) while simultaneously increasing the driving shear stresses acting on the soil. This would result in an initial increase in soil strain potential for larger values of α up to a point after which the shear strain potential becomes constant and subsequently reduces (Kammerer et al. 2003). Hence, shear-induced strains should initially increase as α increases. After reaching a plateau, an increase in α may actually increase the soil's resistance to additional disturbance and strain accumulation beneath the foundation.

Building Height/Width Ratio

Structures with larger building H/B ratios have a greater tendency for tilting and rotational failure, because of their larger dynamic overturning moments. Thus, increasing H/B of a building will amplify SSI-induced shear stresses and the resulting induced shear strains and soil disturbance, which in turn increases the relative contribution of SSI-induced pore pressure generation and settlement. In a less dramatic manner, increasing H/B will increase the volumetric strains that are affected by more extensive softening in the foundation soil (ϵ_{p-SED} and ϵ_{p-CON}) and higher transient hydraulic gradients near the edges of the footing (ϵ_{p-DR}).

Building Weight

An increase in building weight is synonymous to an increase in its contact pressure for the same foundation area. Sand's cyclic strength as well as its resistance to pore pressure generation and liquefaction tend to increase under the higher confining pressure of a structure for all values of D_r . However, if the shaking is strong enough to overcome this higher resistance, larger excess pore pressures may be generated under the structure compared to the free-field, intensifying most of the mechanisms of settlement identified in this study. In terms of strength and stress ratios, sand's cyclic resistance ratio (CRR) tends to decrease under higher confinement for D_r values of greater than 30% (Vaid and Sivathayalan 1996), and sand's cyclic stress ratio (CSR) generally decreases under higher confinement. However, heavier structures experience larger cyclic shear stresses and moments, which should intensify SSI-induced shear stresses, excess pore pressures, and deformations. As a result, the influence of building weight on various mechanisms of settlement is complex, highly site-specific, and dependent on the properties of soil, structure, and ground motion.

3D Drainage

The effective 3D hydraulic conductivities within the foundation soil can influence various modes of seismically induced building settlement in a complex manner. A sand layer with a greater 3D drainage capacity (i.e., sand with a higher effective hydraulic conductivity leading to easier drainage both laterally and vertically) limits the development of excess pore pressures and its tendency to liquefy and to subsequently undergo sedimentation. However, more efficient drainage leads to faster fluid migrations, increasing localized volumetric strains due to partially drained cyclic loading. Conversely, more efficient drainage would shorten the period in which the soil remains in a softened state, increasing the soil's resistance to static shear-type deformations (ϵ_{q-BC}). The influence of drainage on SSI-induced shear deformations (ϵ_{q-SSI}) is more complex due to the complex influence of soil strength loss on the building cyclic inertial forces.

Conclusions

Engineers often estimate liquefaction-induced building settlement using procedures developed to evaluate postearthquake volumetric reconsolidation strains in the free-field. These procedures cannot possibly capture liquefaction-induced building settlement, because they ignore partial drainage that occurs during strong shaking and the important deviatoric strain mechanisms that this testing program has shown to be important. Moreover, the centrifuge test results showed that building settlement is not proportional to the thickness of the liquefiable layer. Therefore, normalizing building settlements by the thickness of the liquefiable layer is misleading and should be avoided.

Buildings started to settle after one significant ground-motion loading cycle in an approximately linear manner with respect to time, quickly surpassing free-field ground settlements. Significant transient excess pore water pressures developed during earthquake shaking and water flowed both laterally and vertically in response to these high hydraulic gradients. SSI-induced cyclic inertial forces also amplified cyclic pore pressure-induced softening directly under the foundations. Pore pressure generation reduced the stiffness and strength of soils beneath the shallow foundations, which also made static bearing-induced shearing of the soil important. Building settlement rates slowed down dra-

matically after strong shaking ceased, indicating that volumetric strains due to reconsolidation of the softened soil are relatively less important. Static and dynamic deviatoric-induced movements in combination with sedimentation and localized volumetric strains due to partial drainage during earthquake shaking were responsible for most of building settlements measured in these experiments. The relative importance of these settlement mechanisms is expected to depend strongly on the properties of the ground motion, soil, and structure.

Centrifuge experiments showed significant ground settlements occurring in the free-field during shaking, indicating partial drainage for this case as well. Settlements in the free-field were controlled by volumetric deformations, which primarily involved the sedimentation- and consolidation-induced settlement mechanisms during and after strong shaking as well as volumetric strains due to partially drained loading (i.e., ε_{p-SED} , ε_{p-CON} , and ε_{p-DR}).

These centrifuge experiments helped identify the dominant settlement mechanisms involved in liquefaction-induced building settlement. The experiments illustrated the complex interactions between key parameters, soil softening, settlement mechanisms, and settlement patterns, and allowed the relative influence of some key parameters to be assessed. An improved understanding of the mechanisms involved in liquefaction-induced building settlement is required to advance the capabilities of numerical simulations and design engineering procedures. Effective mitigation techniques can then be developed that suppress the dominant building settlement mechanisms.

Acknowledgments

This material is based upon work supported by the National Science Foundation (NSF) under Grant No. CMMI-0530714. Any opinions, findings, and conclusions or recommendations expressed in this material are those of the writers and do not necessarily reflect the views of the NSF. Operation of the large geotechnical centrifuge at UC Davis is supported by the NSF George E. Brown, Jr. Network for Earthquake Engineering Simulation (NEES) program under Award No. CMMI-0402490. The writers would also like to thank those at the UC Davis Center for Geotechnical Modeling, and in particular Dr. Bruce Kutter, for their assistance.

References

- Adachi, T., Iwai, S., Yasui, M., and Sato, Y. (1992). "Settlement and inclination of reinforced concrete buildings in Dagupan City due to liquefaction during the 1990 Philippine earthquake." *Proc., 10th World Conf. on Earthquake Engineering*, International Association for Earthquake Engineering (IAEE), Madrid, Spain, 147–152.
- Adalier, K. (1992). "Post-liquefaction behavior of soil systems." MS thesis, Rensselaer Polytechnic Institute, Troy, N.Y.
- Adalier, K., and Elgamal, A. (2005). "Liquefaction of over-consolidated sand: A centrifuge investigation." *J. Earthquake Eng.*, 9(1), 127–150.
- Arulmoli, K., Muraleetharan, K. K., Hossain, M. M., and Fruth, L. S. (1992). "VELACS: Verification of liquefaction analyses by centrifuge studies, Laboratory Testing Program." *Soil Data Report Project No. 90-0562*, The Earth Technology Corporation, Irvine, Calif.
- Dobry, R., and Liu, L. (1992). "Centrifuge modeling of soil liquefaction." *Proc., 10th World Conf. on Earthquake Engineering*, International Association for Earthquake Engineering (IAEE), Madrid, Spain, 7801–6809.
- Elgamal, A. W., Dobry, R., and Adalier, K. (1989). "Small scale shaking table tests of saturated layered sand-silt deposits." *2nd U.S.-Japan Workshop on Soil Liquefaction Rep. No. 89-0032*, NCEER, Buffalo, N.Y., 233–245.
- Fiegel, G.L., and Kutter, B.L. (1994). "Liquefaction-induced lateral spreading of mildly sloping ground." *J. Geotech. Engrg.*, 120(12), 2236–2243.
- Hausler, E. A. (2002). "Influence of ground improvement on settlement and liquefaction: A study based on field case history evidence and dynamic geotechnical centrifuge tests." Ph.D. thesis, Univ. of California, Berkeley, Chap. 5, 271.
- Ishihara, K., and Yoshimine, M. (1992). "Evaluation of settlements in sand deposits following liquefaction during earthquakes." *Soils Found.*, 32(1), 173–188.
- Jafarzadeh, F., and Yanagisawa, E. (1995). "Settlement of sand models under unidirectional shaking." *Proc., 1st Int. Conf. on Earthquake Geotech. Eng.*, Vol. 2, IS-, Tokyo, 693–698.
- Kammerer, A. M., Pestana, J. M., and Seed, R. B. (2003). "Behavior of Monterey 0/30 sand under multidirectional loading conditions." *Geomechanics 2003: Testing, modeling and simulation, Proc., 1st Japan-U.S. Workshop on Testing, Modeling, and Simulation*, Boston, ASCE GSP 143, 154–173.
- Kokusho, T. (1999). "Water film in liquefied sand and its effect on lateral spread." *J. Geotech. Geoenviron. Eng.*, 125(10), 817–826.
- Kulasingham, R., Malvick, E. J., Boulanger, R. W., and Kutter, B. L. (2004). "Strength loss and localization at silt interlayers in slopes of liquefied sand." *J. Geotech. Geoenviron. Eng.*, 130(11), 1192–1202.
- Liu, L., and Dobry, R. (1997). "Seismic response of shallow foundation on liquefiable sand." *J. Geotech. Geoenviron. Eng.*, 123(6), 557–567.
- Martin, G. R., Seed, H. B., and Finn, W. D. L. (1975). "Fundamentals of liquefaction under cyclic loading." *J. Geotech. Engrg.*, 101(5), 423–438.
- Nagase, H., and Ishihara, K. (1988). "Liquefaction-induced compaction and settlement of sand during earthquakes." *Soils Found.*, 28(1), 65–76.
- Pestana, J. M., Hunt, C., and Goughnour, R. (1997). "FEQDRAIN: A finite element program for the analysis of the generation and dissipation of porewater pressure in layered sand deposits." *EERC Research Rep. No. 97-17*, Univ. of California, Berkeley, Calif.
- Sancio, R., Bray, J. D., Durgunoglu, T., and Onalp, A. (2004). "Performance of buildings over liquefiable ground in Adapazari, Turkey." *Proc., 13th World Conf. on Earthquake Engineering*, St. Louis, Mo., Canadian Association for Earthquake Engineering, Vancouver, Canada, Paper No. 935.
- Sawada, S., Tsukamoto, Y., and Ishihara, K. (2006). "Residual deformation characteristics of partially saturated sandy soils subjected to seismic excitation." *Soil Dyn. Earthquake Eng.*, 26(2–4), 175–182.
- Stewart, D. P., Chen, Y. R., and Kutter, B. L. (1998). "Experience with the use of methylcellulose as a viscous pore fluid in centrifuge models." *ASTM Geotech. Test. J.*, 21(4), 365–369.
- Tokimatsu, K., Kojima, J., Kuwayama, A. A., and Midorikawa, S. (1994). "Liquefaction-induced damage to buildings I 1990 Luzon Earthquake." *J. Geotech. Engrg.*, 120(2), 290–307.
- Tokimatsu, K., and Seed, H. B. (1987). "Evaluation of settlements in sands due to earthquake shaking." *J. Geotech. Engrg.*, 113(8), 861–878.
- Vaid, Y. P., and Eliadorani, A. (1998). "Instability and liquefaction of granular soils under undrained and partially drained states." *Can. Geotech. J.*, 35(6), 1053–1062.
- Vaid, Y. P., and Sivathayalan, S. (1996). "Static and cyclic liquefaction potential of Fraser Delta sand in simple shear and triaxial tests." *Can. Geotech. J.*, 33, 281–289.
- Wu, J., Seed, R. B., and Pestana, J. M. (2003). "Liquefaction triggering and post liquefaction deformations of Monterey 0/30 Sand under unidirectional cyclic simple shear loading." *GeoEngrg. Res. Rep. No. UCB/GE/2003-01*, Dept. of Civil and Environmental Engineering, Univ. of California, Berkeley.
- Yoshimi, Y., and Tokimatsu, K. (1977). "Settlement of buildings on saturated sand during earthquakes." *Soils Found.*, 17(1), 23–38.